

# Novel Biodegradable Aliphatic Poly(butylene Succinate-co-cyclic carbonate)s Bearing Functionalizable Carbonate Building Blocks: II. Enzymatic Biodegradation and in Vitro Biocompatibility Assay

Jing Yang,<sup>†</sup> Weisheng Tian,<sup>‡</sup> Qiaobo Li,<sup>†</sup> Yang Li,<sup>†</sup> and Amin Cao<sup>\*,†</sup>

Polymer Materials Laboratory, Modern Synthetic Chemistry Laboratory, Shanghai Institute of Organic Chemistry (SIOC), Chinese Academy of Sciences, 354 Fenglin Road, Shanghai 200032, P. R. China

Received May 18, 2004; Revised Manuscript Received July 19, 2004

In a previous study, we have reported chemical synthesis of novel aliphatic poly(butylene succinate-co-cyclic carbonate) P(BS-co-CC)s bearing various functionalizable carbonate building blocks, and this work will continue to present our new studies on their enzymatic degradation and in vitro cell biocompatibility assay. First, enzymatic degradation of the novel P(BS-co-CC) film samples was investigated with two enzymes of lipase B *Candida Antartica* (Novozyme 435) and lipase *Porcine Pancreas* PPL, and it was revealed that copolymerizing linear poly(butylene succinate) PBS with a functionalizable carbonate building block could remarkably accelerate the enzymatic degradation of a synthesized product P(BS-co-CC), and its biodegradation behavior was found to strongly depend on the overall impacts of several important factors as the cyclic carbonate (CC) comonomer structure and molar content, molar mass, thermal characteristics, morphology, the enzyme–substrate specificity, and so forth. Further, the biodegraded residual film samples and water-soluble enzymatic degradation products were allowed to be analyzed by means of proton nuclear magnetic resonance (<sup>1</sup>H NMR), gel permeation chromatograph (GPC), differential scanning calorimeter (DSC), attenuated total reflection FTIR (ATR-FTIR), scanning electron microscope (SEM), and liquid chromatograph-mass spectrometry (LC-MS). On the experimental evidences, an exo-type mechanism of enzymatic chain hydrolysis preferentially occurring in the noncrystalline domains was suggested for the synthesized new P(BS-co-CC) film samples. With regard to their cell biocompatibilities, an assay with NIH 3T3 mouse fibroblast cell was conducted using the novel synthesized P(BS-co-CC) films as substrates with respect to the cell adhesion and proliferation, and these new biodegradable P(BS-co-CC) samples were found to exhibit as low cell toxicity as the PLLA control, particularly the two samples of poly(butylene succinate-co-18.7 mol % dimethyl trimethylene carbonate) P(BS-co-18.7 mol % DMTMC) and poly(butylene succinate-co-21.9 mol % 5-benzyloxy trimethylene carbonate) P(BS-co-21.9 mol % BTMC) were interestingly found to show much better cell biocompatibilities than the PLLA reference.

## Introduction

In recent years, biodegradable polymers have played increasingly important roles in the biomedical and pharmaceutical application fields, mainly including drug delivery systems (DDS), artificial implants, and functional materials for tissue engineering and organ regeneration.<sup>1–5</sup> As one of the most important class of synthetic biodegradable polymers, aliphatic polyesters have been focused due to the favorable nature that they can be degraded into less or nontoxic water-soluble mass and further be metabolized or eliminated under the micro-environment in vivo.<sup>6–8</sup> Alternatively, aliphatic poly(carbonate) has been known as another category of synthetic biodegradable polymers with good processability and enough flexibility in designing molecular functionality,

degradation behavior and physical properties, thus become a new crucial class of biomaterials.<sup>9</sup>

So far, high molecular weight aliphatic polyester of poly(butylene succinate) PBS has nowadays been known as an important commercialized biodegradable polymer derived from renewable fatty C-4 compounds.<sup>10–12</sup> Because of the features of its highly hydrophobic macromolecular architecture and less functionality for post-modification, up to date, there were few works on exploring possible applications of PBS and its copolymers as new biomaterials. On the other hand, it has been known that copolymerization becomes a very important strategy to create new biomedical materials with a wide variety in the biodegradation behavior and mechanical performance. For instance, to copolymerize trimethylene carbonate (TMC) monomer with  $\epsilon$ -caprolactone, glycolide, D/L-lactide comonomers etc, morphologies of the synthesized materials were found to strongly depend on their comonomer compositions, and a substantial increase in degradation rate could be readily tuned by incorporating ester

\* To whom correspondence should be addressed. Phone: +86-21-6416-7152. Fax: +86-21-6416-6128. E-mail: acao@mail.sioc.ac.cn.

<sup>†</sup> Polymer Materials Laboratory.

<sup>‡</sup> Modern Synthetic Chemistry Laboratory.

functionality.<sup>13–16</sup> Kimura et al.<sup>17</sup> reported that the introduction of a small amount (3 mol %) of L-lactate repeating units into the PBS polymer chains could result in an increase in molecular weight of the final PBSL copolyester products and concurrently imparting chain hydrolytic instability, and the lipase catalyzed degradation of these PBSL copolymer fibers showed biodegradability much better than that of the PBS. Furthermore, studies on new biodegradable and biocompatible polymers bearing various pendant substituents are now of particular interest because these additional pendant functionalities could be well tailored to tune not only the physical properties and biodegradation behavior but functionalizable sites opening for carrying covalently bonded bioactive molecules and creation of novel functional polyplexes for biomedical purposes.<sup>18–20</sup>

When screening a new biodegradable polymer as possible biomaterial, an additional assay of biocompatibility and cytotoxicity according to the generalized guideline has routinely been known as a critical and efficient step, and the living cell toxicity test is the initial phase in exploring the biocompatibility of potential biomaterials and biomedical devices.<sup>21–23</sup> In the case of novel biodegradable copolymers, the cytotoxicity might be commonly from three possible origins: the first part can be attributed to the degraded intermediate compounds and the final degradation products; a second part includes the trace amount of toxic catalyst residues; the third origin could come from any substances which would leach from the bulk copolymers since the low molecular weight components have been reported to exhibit different levels of physiologic activity and living cell toxicity.<sup>24</sup>

In our recent works,<sup>25</sup> we reported the chemical synthesis of novel chiral biodegradable aliphatic poly(butylene succinate-*co*-butylene malate)s and poly(butylene succinate-*co*-cyclic carbonate)s with functionalizable carbonate building blocks. For a linear biodegradable polyester or poly(ester carbonate), the presence of lateral functionality such as hydroxyl functional site could bring many benefits as follows: (i) It can easily adjust hydrophilic/hydrophobic balance of a material via regulating the hydrophilic lateral group and the hydrophobic chain backbone, and this would result in a variety of interesting condense states such as the macromolecular self-assembled cylinder or core-shell shaped morphologies as reported.<sup>26</sup> (ii) A further attachment of a bioactive molecule such as indomethacin to the functional sites could construct a new polymer drug with well controlled release.<sup>27</sup> (iii) Via cross-linking of the pendant functionalities, new biodegradable polymer network could be synthesized as drug and/or possible catalyst carrier. (iv) A further living/controlled ring opening polymerization of reactive cyclic monomer grafted at the reactive hydroxyl sites could construct a functional brush- or comb-type polymer architecture through controlling the graft density and length.<sup>28</sup>

On the basis of the previous work of chemical synthesis and physical characterization of new biodegradable P(BS-*co*-CC)s bearing functionalizable building blocks,<sup>25b</sup> in this study, we continuously investigated their enzymatic degradation behavior, in vitro biocompatibility and possibility as a new biodegradable polymer drug carrier. First, the lipases

Novozyme 435 and PPL catalyzed degradation behavior were studied for the synthesized copolymer film samples in terms of molecular weight, comonomer molar content, thermal characteristics and morphologies by means of proton nuclear magnetic resonance (<sup>1</sup>H NMR), gel permeation chromatograph (GPC), differential scanning calorimeter (DSC), attenuated total reflection FTIR (ATR-FTIR), and scanning electron microscope (SEM). Furthermore, the water-soluble enzymatic degradation products were analyzed by <sup>1</sup>H NMR and liquid chromatograph-mass spectrometry (LC-MS). Finally, NIH 3T3 mouse fibroblast cells were applied to have an in vitro cell biocompatibility assay via the 3-(4,5-dimethylthiazol-2-yl)-2,5-diphenyltetrazolium bromide (MTT) method using the P(BS-*co*-CC) films as the cell cultivation substrates.

## Experimental Section

**Materials.** Novel biodegradable aliphatic poly(butylene succinate-*co*-cyclic carbonate)s P(BS-*co*-CC)s bearing functionalizable carbonate building blocks, namely poly(butylene succinate-*co*-trimethylene carbonate)s P(BS-*co*-TMC), poly(butylene succinate-*co*-1-methyl-1,3-trimethylene carbonate)s P(BS-*co*-MTMC), poly(butylene succinate-*co*-2,2'-dimethyl-1,3-trimethylene carbonate)s P(BS-*co*-2,2'-DMTMC), poly(butylene succinate-*co*-5-benzyloxy trimethylene carbonate)s P(BS-*co*-BTMC), and poly(butylene succinate-*co*-5-ethyl-5'-benzyloxymethyl trimethylene carbonate)s P(BS-*co*-EBTMC), were synthesized with various carbonate unit molar contents as described in a previous work, meanwhile their physical properties were thereby characterized.<sup>25b</sup> Here, their molecular characteristics and physical properties were summarized in Table 1. In this study, the porous poly(acrylic acid) immobilized lipase B Candida Antartica (Novozyme 435) was gifted by Novozymes Co. Ltd, China with a specific activity of 10000 PLU/g, and another kind of lipase from Porcine Pancreas PPL EC(3.1.1.3) was purchased from Sigma with a specific activity of 41 units/mg. Additionally, PLLA (*M<sub>w</sub>* = 300 KDa) was kindly provided by Mr. X. Pan of Synica Co. Ltd, Shanghai. Fetal bovine serum (FBS), penicillin, streptomycin, NIH 3T3 mouse fibroblast cell strain, 3-(4,5-dimethylthiazol-2-yl)-2,5-diphenyltetrazolium bromide (MTT) and other chemicals and solvents commercially supplied in China were utilized without further purification.

**Lipase Catalyzed In Vitro Biodegradation.** Each P(BS-*co*-CC) film sample was hot-pressed with a predetermined thickness of 0.12 mm ± 0.01 mm via a stainless spacer at a processing temperature of 25 ~ 30 °C above its corresponding melting temperature and a pressure of 20 ~ 25 MPa (Imoto Ltd. Japan). The hot-pressed films were in turn extensively rinsed with ethanol and distilled water and dried in vacuum oven, and then stored at the room temperature for at least 1 week in order to approach the equilibrium crystallinity prior to use. These clean film samples with initial dimension of 30 × 10 mm<sup>2</sup> and initial weight of about 20 ~ 30 mg were incubated in triplicate in vials containing 4.0 mL of 0.06 M phosphate buffering solution (pH = 7.4, Na<sub>2</sub>HPO<sub>4</sub> and NaH<sub>2</sub>PO<sub>4</sub> in 0.9% NaCl solution) in the presence

**Table 1.** Characteristics of the Novel Synthesized Biodegradable P(BS-co-CC)s Bearing Various Functionalizable Carbonate Building Blocks

no.	sample <sup>a</sup>	carbonate unit content (mol %) <sup>b</sup>	molecular weight <sup>c</sup>		<i>T<sub>m</sub></i> <sup>d</sup> (°C)	<i>DH<sub>m</sub></i> <sup>d</sup> (J/g)
			<i>M<sub>n</sub></i> (10 <sup>-4</sup> g/mol)	<i>M<sub>w</sub></i> / <i>M<sub>n</sub></i>		
1	P(BS-co-17.4 mol % TMC)	17.4	4.53	2.60	84.7	56.1
2	P(BS-co-26.5 mol % TMC)	26.5	6.08	3.33	88.6	40.3
3	P(BS-co-28.6 mol % TMC)	28.6	6.73	3.51	64.3	22.5
4	P(BS-co-11.5 mol % MTMC)	11.5	3.25	3.77	105.3	53.2
5	P(BS-co-16.7 mol % MTMC)	16.7	9.96	2.71	79.3	40.9
6	P(BS-co-13.0 mol % DMTMC)	13.0	4.19	4.55	94.1	49.5
7	P(BS-co-18.7 mol % DMTMC)	18.7	6.08	4.74	85.9	36.2
8	P(BS-co-6.5 mol % BTMC)	6.5	5.91	3.87	103.6	52.1
9	P(BS-co-13.0 mol % BTMC)	13.0	5.64	4.51	79.9	29.8
10	P(BS-co-21.9 mol % BTMC)	21.9	4.24	3.67	56.9	17.2
11	P(BS-co-7.4 mol % EBTMC)	7.4	2.43	3.58	99.7	51.3
12	P(BS-co-25.9 mol % EBTMC)	25.9	4.28	5.97	46.7	6.7
13	PBS	0	5.69	3.29	112.4	54.5

<sup>a</sup> Chemical synthesis of these samples has already been reported in ref 25b. <sup>b</sup> The carbonate unit molar contents were evaluated by <sup>1</sup>H NMR. <sup>c</sup> Molecular weights were measured by GPC in CHCl<sub>3</sub> with PS standards. <sup>d</sup> Melting point and heat of fusion were measured by DSC at 20 °C/min (first heating scan) after reaching the crystallinity equilibrium.

of a chosen enzyme. The vials were sealed with aluminum caps and transferred into a thermostated chamber at 37.0 ± 0.1 °C with reciprocal shaking. From triggering the biodegradation experiment, the reaction buffer solution was refreshed every 40 h to keep the enzymatic activity. After a predetermined period of incubation, the film samples were taken out and well rinsed with ion exchanged water, and dried to the constant weight in vacuum oven at the room temperature. With regard to the biodegradability assay, the lipase catalyzed biodegradation behavior was accordingly characterized on the weight loss normalized by the initial sample surface area,<sup>29</sup> molecular weight, thermal characteristics and the surface morphology of each film sample before and after the degradation experiment. Here, the film surface area exposed to enzymatic attacking was presumed as a sum area (6.0 cm<sup>2</sup>) of double sides, and it was supposed to keep constant during the biodegradation to simplify the characterization. Furthermore, the water-soluble enzymatic degradation products were collected and then filtered through a microporous membrane to remove the enzyme and water-insoluble substances, and the filtrate was lyophilized and thus analyzed by <sup>1</sup>H NMR and LC-MS.

**In Vitro Cell Biocompatibility Assay. Cell Cultivation.** Mouse fibroblast cells of NIH 3T3 strain were propagated in a RPMI 1640 medium, including 10% fetal bovine serum (FBS), 1% double antibiotics containing 100 IU/mL penicillin, and 100 µg/mL streptomycin, and the cells were cultivated at 37 °C in the humidified atmosphere of 5% carbon dioxide in air.

**Cell Biocompatibility Assay.** The clean polymer film samples were cut into circular pieces with a diameter of 14 mm and, in turn, sterilized with 75% ethanol and further rinsed with phosphate buffer solution, and finally placed into 24-well nontreated culture plates with the circular pieces of commercially available PLLA as control. The cells of the NIH 3T3 strain were seeded onto the substrates with an initial density of 1 × 10<sup>7</sup> cells per well and incubated for 48 h at 37 °C under 5% CO<sub>2</sub>. Thereafter, the cell morphology and adhesion were monitored by an Optimas 5.2 image analysis system (Optimas Ltd., USA) attached to an IX 70 inverted

phase contrast microscope (Olympus Ltd, Japan) via a Nikon digital camera.

**MTT Cytotoxicity Assay.** First, cells of the NIH 3T3 strain were seeded on the 24-well plates (density: 1.0 × 10<sup>7</sup>/well) and incubated at 37 °C in a humidified atmosphere of 5% carbon dioxide for 48 h. Then, 40 µL of MTT and 360 µL of culture medium solution were added into each well and further incubated for 6 h. Then, the medium-sample MTT solution was aspirated, and 300 µL of DMSO was added into each well. Shaking the microtiter plate for 15 min to solubilize the formazan product, 180 µL of the supernatant of each well was transferred to a new microtiter plate, and the absorbance of the solutions was measured with a microplate photometer at a wavelength of 550 nm. Four wells for each sample were used for the statistical analysis.

**Statistical Analysis.** All of the data were analyzed by one-way factorial ANOVA and multiple comparisons. Mean value and standard deviation were given for all samples. A paired two-tailed *t*-test was used for two sample comparisons. A difference was taken to be significant if *p* < 0.05.

**Analytical Procedures. Molecular Weight Characterization.** Molecular weights were measured under 40 °C on a Perkin-Elmer 200 series of gel permeation chromatography (GPC) equipped with double PLgel 5µm mixed-D type of 300 × 7.5 mm columns set in series (PolyLab Ltd., U.K.). Chloroform was employed as the eluant at a flowing rate of 1.0 mL/min. Molecular weights (*M<sub>w</sub>*, *M<sub>n</sub>*) and polydispersity indexes (*M<sub>w</sub>*/*M<sub>n</sub>*) were evaluated for each polymer sample with a commercial polystyrene calibration kit purchased from Showa Denko Co. Ltd., Japan.

**Thermal Analysis.** DSC measurements were implemented under nitrogen atmosphere on a Perkin-Elmer Pyris 1 differential scanning calorimeter (DSC). Metal indium was applied as the external standard for calibration of temperature and heat of fusion. Each sample of about 3 mg was pre-sealed in an aluminum pan, and DSC trace was scanned from 25 to 120 °C at a rate of 20 °C/min. Melting point (*T<sub>m</sub>*) and heat of fusion (*ΔH<sub>m</sub>*) were evaluated as the corresponding main peak top temperature and integral of the DSC endothermic trace in the first heating scan, respectively.



**NMR Measurement.** A Varian VXR 300 Fourier transform nuclear magnetic resonance (NMR) spectrometer was utilized for analysis of the lipase catalyzed water-soluble biodegradation products and film samples before and after degradation test. NMR measurements were conducted under ambient temperature in corresponding  $\text{CDCl}_3$  or  $\text{D}_2\text{O}$  solution, and tetramethylsilane (TMS) was applied as an internal chemical shift reference for the NMR analysis in  $\text{CDCl}_3$ .

**Film Surface Analysis.** Surface analysis of the biodegraded film samples were performed via an attenuated total reflection Fourier transform infrared spectrometer (ATR-FTIR). In this study, all ATR-FTIR measurements were measured at ambient temperature with a KRS-5 crystal instrumental unit at a nominal incident angle of  $45^\circ$ . Film samples were cut into ATR crystal size ( $10 \text{ mm} \times 80 \text{ mm}$ ) and mounted onto the side of the trapezoid crystal. The ATR-FTIR spectroscopy was measured on a Nicolet AV-360 spectrometer with an average of over 32 scans and a resolution of  $4 \text{ cm}^{-1}$ . Alternatively, film morphologies of the enzymatic degraded samples were examined with a JEOL JSM-5600LV scanning electron microscope (SEM), and all samples were mounted on metal stubs and preparatively sputter-coated with gold–palladium (Denton Vacuum Desc II).

**LC-MS Analysis of Water Soluble Degradation Products.** The liquid chromatography–mass spectrometry (LC-MS) apparatus was employed for quantitative analysis of the water-soluble enzymatic degradation products. LC-MS measurements were conducted on an Agilent LCMSD SL system (Agilent Technologies, U.S.A.) attached with a binary pump, solvent degasser, column compartment, diode-array detector (DAD) and quadrupole mass spectrometer. A reversed column of Inertsil ODS-3 (GL Science Inc.) was used. The mobile phase for LC analysis was 0.1% acetic acid/acetonitrile (70:30, v/v %) at a flowing rate of  $0.5 \text{ mL/min}$ , and the mass spectra were recorded by an electro-spray ionization probe.

## Results and Discussion

**Biodegradation of the Synthesized P(BS-co-CC)s by Lipases Novozyme-435 and PPL.** Commonly, enzymatic degradation has been known as a convenient way to preliminarily examine the possible bioactivity of a synthetic polymer material. In this study, 12 novel synthesized copolymer samples as reported in a previous work<sup>25b</sup> were subjected to the attack of enzyme molecules for characterization of their biodegradation behavior. First, a necessary test was conducted to investigate the lipase-concentration dependence of enzymatic degradation behavior. 5 samples of poly(butylene succinate-co-26.5mol % trimethylene carbonate) P(BS-co-26.5mol %TMC), poly(butylene succinate-co-16.7mol %-1-methyl-1,3-trimethylene carbonate) P(BS-co-16.7 mol % MTMC), poly (butylene succinate-co-18.7 mol %-2,2'-dimethyl-1,3-trimethylene carbonate) P(BS-co-18.7 mol % DMTMC), poly (butylene succinate-co-21.9mol %-5-benzyloxy trimethylene carbonate)s P(BS-co-21.9 mol % BTMC) and poly(butylene succinate-co-7.4 mol %-5-ethyl-5-benzyloxymethyl trimethylene carbonate)s P(BS-co-7.4 mol %EBTMC) bearing distinct carbonate building blocks were chosen as models of 5 series of P(BS-co-CC)s. Film

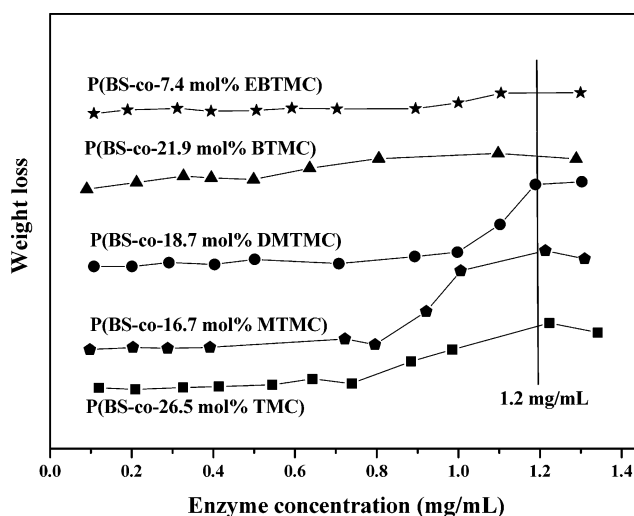


**Figure 1.** Enzyme concentration dependence of film weight loss for 5 kinds of P(BS-co-CC)s bearing distinct carbonate building blocks for Lipase Novozyme 435 after 40 h degradation.

samples of each copolymer were incubated in vials at  $37^\circ\text{C}$  for 40 h in the presence of lipase Novozyme 435 under various concentrations.

Figure 1 depicts the results of the normalized weight loss of film sample as a function of lipase concentration. Increasing the enzyme concentration, the 5 kinds of P(BS-co-CC) samples tended to initially degrade in a slow manner, and when the lipase concentration became higher than  $800 \mu\text{g/mL}$ , the apparent enzymatic degradation rates increased remarkably, indicating an obvious enzyme-concentration dependence of biodegradation. Thus, a feasible experimental condition of lipase concentration equal to  $1.2 \text{ mg/mL}$  was tentatively applied for study of biodegradabilities of these synthesized poly(ester carbonate)s. In parallel, degradation of these P(BS-co-CC) samples was studied in the same buffer solution without any enzyme as controls, and negligible weight loss of film could be detected even after an incubation time of 1000 h. Hence, the results of blank samples substantiated the considerable stabilities of copolymers against hydrolysis under the above test conditions.

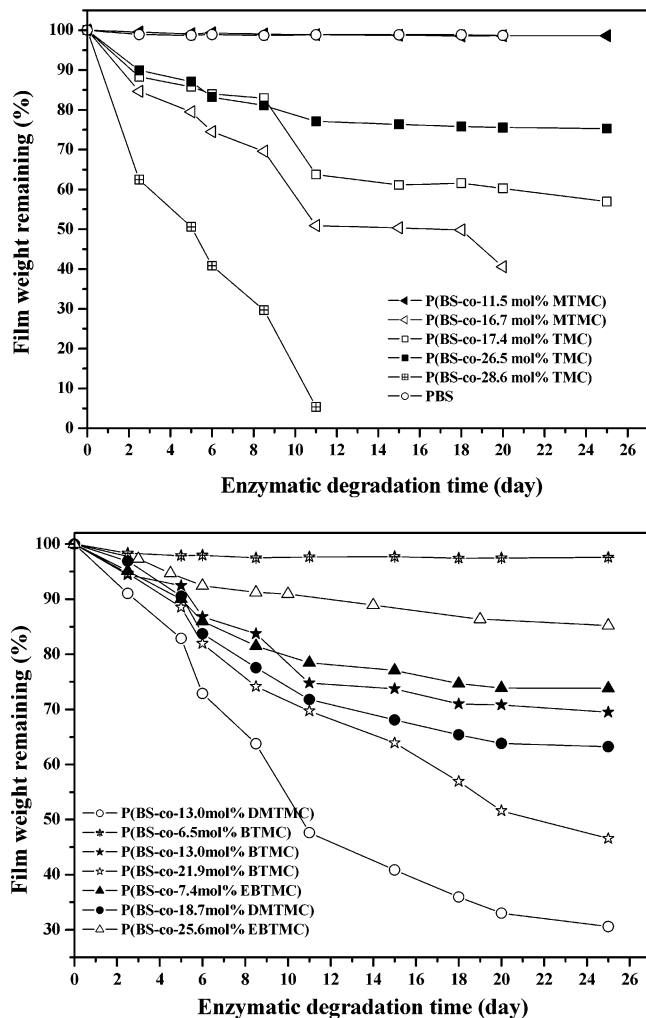
Figure 2 shows the results of enzymatic degradation of 12 P(BS-co-CC) samples bearing various functionalizable carbonate building blocks of TMC, MTMC, DMTMC, BTMC, and EBTMC as well as poly(butylene succinate) PBS and were further plotted as the percentage of weight remaining of film samples vs the incubation time. As for PBS, approximately there was not any appreciable weight loss detected even after an incubation time scale of 25 days, and similar results could also be seen for two copolymers of P(BS-co-6.5 mol % BTMC) and P(BS-co-11.5 mol % MTMC) upon the attack of lipase Novozyme 435. In contrast, an early stage of rapid degradation was detected for the other copolymer samples bearing various CC building blocks and their different comonomer contents within 12 days after triggering the test experiments, and the enzymatic degradation thereafter tended to proceed in a more gradual manner.

In general, several important factors such as chemical structure of repeating unit, molar mass, degree of crystallinity, thermal characteristics, domains of crystalline and amorphous regions, morphology, and so forth should concur-

**Table 2.** Molecular Weight and Carbonate Comonomer Molar Content Characterized before and after Enzymatic Degradation by Lipase CA (Novozyme 435)

sample	degradation time (day)	sample weight remaining (%)	carbonate molar content (%) <sup>a</sup>	$M_n$ ( $10^{-4}$ g/mol) <sup>b</sup>	$M_w/M_n^b$
P(BS-co-17.4 mol % TMC)	0	100	17.4	4.53	2.60
	25	60	17.0	3.30	2.93
P(BS-co-16.7 mol % MTMC)	0	100	16.7	9.96	2.70
	20	40	15.3	7.41	3.01
P(BS-co-13.0 mol % DMTMC)	0	100	13.0	4.19	4.55
	25	30	12.6	4.43	4.68
P(BS-co-21.9 mol % BTMC)	0	100	21.9	6.07	3.67
	25	45	20.6	5.35	3.71

<sup>a</sup> The carbonate unit molar contents were evaluated by  $^1\text{H}$  NMR. <sup>b</sup> Molecular weight and polydispersity were characterized by GPC in  $\text{CHCl}_3$  with PS standards.

**Figure 2.** Enzymatic degradation of 12 P(BS-co-CC) film samples as well as PBS by lipase Novozyme 435 in phosphate buffer solution at 37 °C (pH = 7.4).

recently affect the apparent enzymatic degradation behavior of a synthetic biodegradable polymer. As seen in Figure 2, increasing the carbonate building block content of a synthesized P(BS-co-CC) finally led to an obvious increase in the enzymatic degradation rate, and an order of enzymatic degradation rate was detected for the series of P(BS-co-BTMC)s with  $\text{P(BS-co-21.9 mol \% BTMC)} > \text{P(BS-co-13.0 mol \% BTMC)} > \text{P(BS-co-6.5 mol \% BTMC)}$ . This result can be readily interpreted for their individual ordered condense structures, i.e., the more CC content in copolymer would

result in significant changes in melting point, degree of crystallinity as well as the sample morphology. A copolymer with less degree of crystallinity would be more prone to the enzyme attack because the chains and/or segments in amorphous domain were reported to have more flexibilities and freedom of movement. On the other hand, the P(BS-co-26.5 mol % TMC) was observed to exhibit an enzymatic degradation rate lower than that of P(BS-co-17.4 mol % TMC), indicating a different tendency as stated above. This might be accounted for a relatively low molar mass  $M_n$  equal to 4.53 KDa and melting point of P(BS-co-17.4 mol % TMC) as compared with P(BS-co-26.5 mol % TMC). Similar abnormal enzymatic degradation rate trend could also be detected for the P(BS-co-DMTMC)s with 13.0 and 18.7 mol % DMTMC, respectively, probably due to the presence of two methyl substitutes in carbonate unit retarding the enzyme attack. On these evidences, to copolymerize linear aliphatic PBS with a functionalizable carbonate building block remarkably accelerated the enzymatic degradation of new synthesized P(BS-co-CC)s, and the factors of molar mass, thermal characteristics, morphology, and chemical structure and so on were found to play important role as the cyclic carbonate (CC) building block molar content. In particular, the apparent enzymatic degradation behavior of P(BS-co-CC)s with similar CC contents should be determined by the overall impacts of these factors.

After the lipase Novozyme 435 catalyzed degradation, the residual water-insoluble mass of film samples were allowed to be further analyzed by means of GPC and  $^1\text{H}$  NMR to reveal the variation in molar mass and comonomer molar composition. Table 2 summarized the results of molar mass and carbonate building block molar content for 4 kinds of P(BS-co-CC) samples, and only slight changes in molar mass and CC content were detected after 20 ~ 25-day enzymatic erosion. Therefore, an exo-type of chain enzymatic degradation could be proposed to occur uniformly from the film sample surface as well reported for biological polyester poly(hydroxyl alkanate)s PHA.<sup>30</sup>

With regard to the water-soluble degradation products, Figure 3 depicts a typical  $^1\text{H}$  NMR spectrum of the water-soluble degradation products in  $\text{D}_2\text{O}$  solution for the P(BS-co-CC)s bearing the carbonate building block of DMTMC, and the proton NMR signals were reasonably assigned to the nuclei locating at different sites. For an easy structural elucidation, some of the possible water-soluble products were

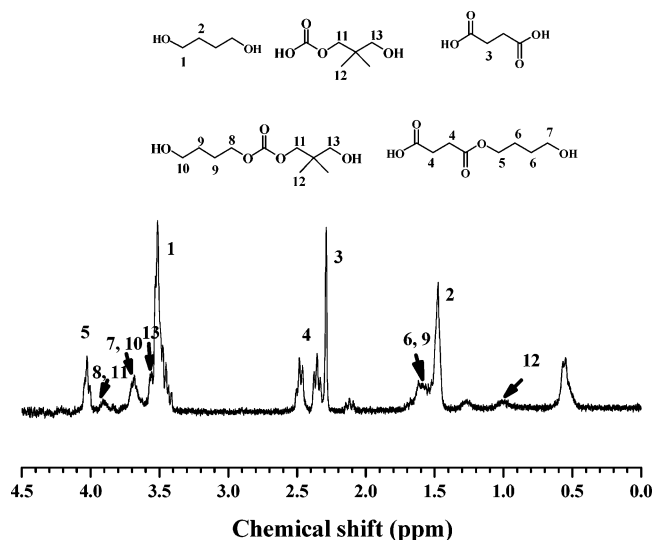
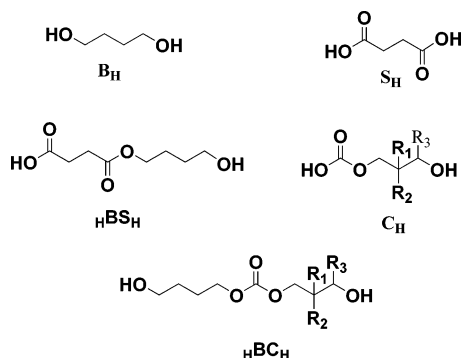


**Figure 3.** Typical  $^1\text{H}$  NMR spectrum for the isolated water-soluble degradation products of P(BS-co-13.0 mol % DMTMC) by lipase Novozyme 435.

**Scheme 1.** Some of the Possible Water-Soluble Degradation Products



denoted for the synthesized P(BS-co-CC)s as shown in Scheme 1. The substances with different degree of polymerization and functional terminal group were here expressed as  $\text{HBSH}$ ,  $\text{HBSBSH}$ ,  $\text{HBCSH}$ ,  $\text{HCSBCH}$ , and so forth, in which the subscript H indicated the terminal functional group as hydroxyl or carboxyl, depending on which of the corresponding three B, S, and C appeared as the terminal unit. As seen in Figure 3, there are two sets of resonance signals respectively occurring at the up (signals 2, 6, and 9) and down (signals 5, 7 or 10, and 8) magnetic fields, implying the presence of final degradation products of  $\text{B}_\text{H}$ ,  $\text{HBSH}$ ,  $\text{HBCSH}$ . The sharp singlet signal 3 at 2.29 ppm suggested the presence of monomeric product  $\text{S}_\text{H}$  along with the substance of  $\text{B}_\text{H}$ . Meanwhile, the characteristic proton resonance signal 12 in Figure 3 were obviously detected for the possible origins of methyl protons in the DMTMC unit, demonstrating the presence of carbonate structural units in the water-soluble degradation products in either monomeric or oligomeric state. Similar results could also be revealed for the water-soluble degradation products of other P(BS-co-CC)s bearing different carbonate building blocks.

On the other hand, to investigate the enzyme dependence of biodegradation, in a similar way, enzymatic degradation was examined for the P(BS-co-CC) film samples with lipase PPL under another tentative concentration of 800  $\mu\text{g/mL}$ . It

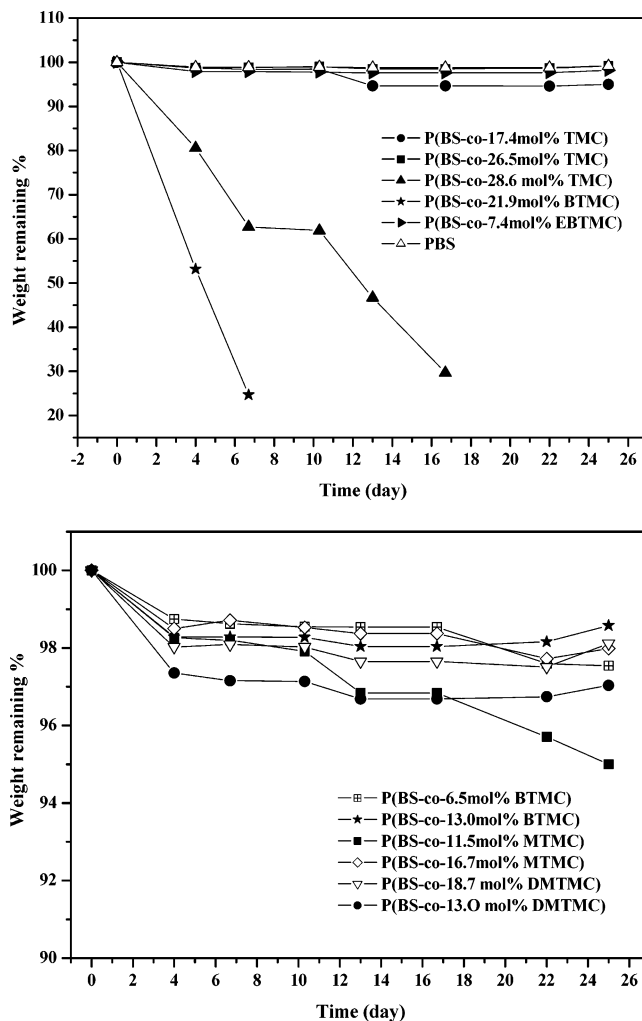


**Figure 4.** Enzymatic degradation of 12 P(BS-co-CC) film samples at 37 °C in phosphate buffer solution (pH = 7.4) by Lipase PPL.

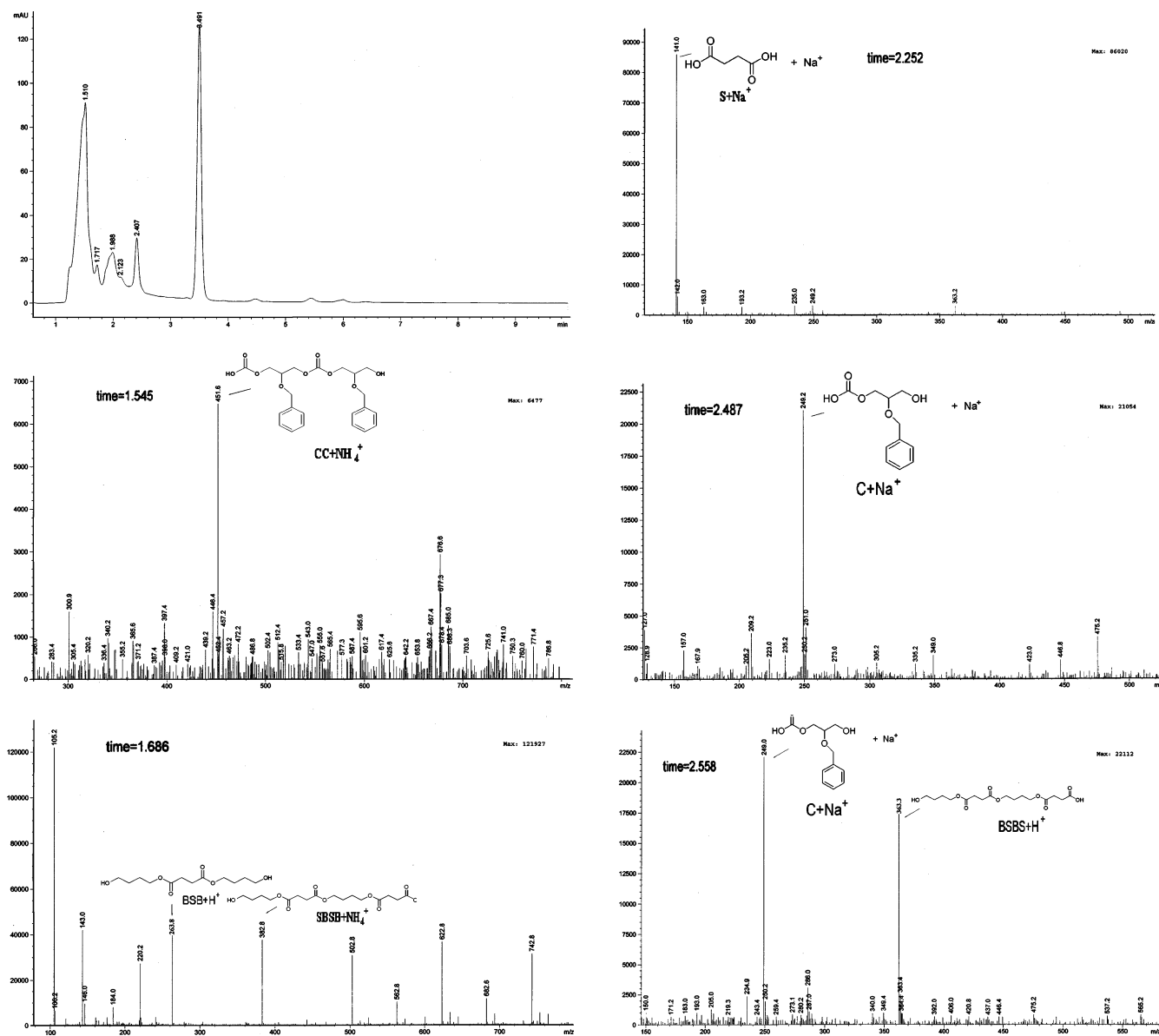
was seen that only two samples of P(BS-co-21.9 mol % BTMC) and P(BS-co-28.6 mol % TMC) exhibited obvious enzymatic degradation as shown in Figure 4 even after a 25-day enzymatic erosion, and there could hardly detect any applicable weight loss for the other 10 copolymer film samples. As compared with enzymatic degradation by lipase Novozyme 435, this result clearly indicated a strong substrate-specificity of lipase PPL on enzymatic degradation of the synthesized P(BS-co-CC)s bearing different carbonate building blocks.

Furthermore, molar mass, polydispersity, comonomer molar content and thermal characteristics of the enzymatically well degraded P(BS-co-21.9 mol % BTMC) film sample were allowed to be characterized by means of GPC,  $^1\text{H}$  NMR and DSC for lipase PPL. As seen in Table 3, the values of  $M_n$  tended to slightly increase along with a tiny decrease in the  $M_w/M_n$  value under various incubation times, and this was suggested for the surface initiated nonspecific biodegradation and loss of low molar mass components, a phenomenon as revealed for the enzyme of lipase Novozyme 435. On the other hand, it was observed that the heat of fusion  $\Delta H_m$  for the enzymatic degraded films of P(BS-co-21.9 mol % BTMC) was found to be higher than those of its original

**Table 3.** Enzymatic Degradation Time Dependence of Characteristics for the P(BS-co-21.9 mol %BTMC) by Lipase PPL

degradation time (h)	remaining weight (%)	$M_n$ ( $10^{-4}$ g/mol) <sup>a</sup>	$M_w/M_n$ <sup>a</sup>	$T_m$ (°C)	$\Delta H_m$ (J/g) <sup>b</sup>	BTMC unit content (mol %) <sup>c</sup>
0	100	4.24	3.70	54.6	17.2	21.9
6	60	4.28	3.67	54.0	20.6	21.7
10	33	4.86	3.26	55.6	23.8	21.3
14	24	5.53	3.11	55.3	22.7	21.0
20	10			55.6	23.1	21.2

<sup>a</sup> Molecular weight and polydispersity were measured by GPC in  $\text{CHCl}_3$  with PS standards. <sup>b</sup> Melting point and heat of fusion were evaluated by DSC at 20 °C/min (the first heating scan). <sup>c</sup> The BTMC unit molar contents were measured by  $^1\text{H}$  NMR.

**Figure 5.** LC-MS analysis of the water-soluble fragments for the P(BS-co-21.9 mol %BTMC) after a 28-day biodegradation by lipase PPL.

sample, indicating that the enzymatic degradation would preferentially occur in the amorphous regions<sup>31–33</sup> and/or less well ordered partially crystallized micro-domains.<sup>34</sup>

To shed a new light on the enzymatic degradation, Figure 5 shows the LC analytical results monitored by a UV detector at 254 and 210 nm for the collected water-soluble products of the P(BS-co-21.9 mol %BTMC) after a 28-day enzymatic degradation by lipase PPL. There were a series of substances detected in a retention time (RT) spanning from 1 to 10 min. Furthermore, the LC-MS signals were further reasonably assigned to the possible water-soluble fragments as sum-

marized in Table 4. The ion at  $m/z = 141.0$  could be assigned to the  $\text{S}+\text{Na}^+$  fragment, and the mass signal at  $m/z = 249.0$  could be attributed to the fragment  $\text{C}_\text{H} + \text{Na}^+$ , where C means the moiety derived from 5-benzyloxy trimethylene carbonate unit (BTMC). In addition, another two ions at  $m/z = 382.8$  and  $451.6$  were thus attributed to the possible fragments of  $\text{SBSB} + \text{NH}_4^+$  and  $\text{CC} + \text{NH}_4^+$ , respectively. These results demonstrated that the predominant water-soluble enzymatic degradation products were monomeric and oligomeric substances for the P(BS-co-CC)s, depending on their different carbonate building blocks.



**Table 4.** LC-MS Analysis of the Water-soluble Enzymatic Degradation Products for the P(BS-*co*-21.9 mol %BTMC) by Lipase PPL

<i>m/z</i>	chemical structure	symbols
141.0	HOOC(CH <sub>2</sub> ) <sub>2</sub> COOH+Na <sup>+</sup>	S+Na <sup>+</sup>
249.0	HOCO <sub>2</sub> CH <sub>2</sub> CH(OCH <sub>2</sub> Ph)CH <sub>2</sub> OH+Na <sup>+</sup>	C+Na <sup>+</sup>
263.8	HO(CH <sub>2</sub> ) <sub>4</sub> OCO(CH <sub>2</sub> ) <sub>2</sub> CO <sub>2</sub> (CH <sub>2</sub> ) <sub>4</sub> OH+H <sup>+</sup>	BSB+H <sup>+</sup>
363.3	HO(CH <sub>2</sub> ) <sub>4</sub> OCO(CH <sub>2</sub> ) <sub>2</sub> COO(CH <sub>2</sub> ) <sub>4</sub> OCO(CH <sub>2</sub> ) <sub>2</sub> COOH+H <sup>+</sup>	BSBS+H <sup>+</sup>
382.8	HOOC(CH <sub>2</sub> ) <sub>2</sub> COO(CH <sub>2</sub> ) <sub>4</sub> OCO(CH <sub>2</sub> ) <sub>2</sub> COO(CH <sub>2</sub> ) <sub>4</sub> OH+NH <sub>4</sub> <sup>+</sup>	SBSB+NH <sub>4</sub> <sup>+</sup>
451.6	HOCO <sub>2</sub> CH <sub>2</sub> CH(OCH <sub>2</sub> Ph)CH <sub>2</sub> OCO <sub>2</sub> CH <sub>2</sub> CH(OCH <sub>2</sub> Ph)CH <sub>2</sub> OH+NH <sub>4</sub> <sup>+</sup>	CC+NH <sub>4</sub> <sup>+</sup>

**Morphological Study of Biodegraded P(BS-*co*-21.9mol %BTMC) Films by Lipase PPL.** Attenuated total reflection FT-IR technique (ATR-FTIR) has been well-known as a useful tool to have a deep study on exploring the structural information to several controllable depths from surface. Regarding to the ATR-FTIR spectra of P(BS-*co*-21.9 mol % BTMC) film samples, there was characteristic absorption detected at about 1714 cm<sup>-1</sup>, and this could be attributed to the carbonyl stretching vibration mode ( $\nu_{C=O}$ ). Thus, all ATR-FTIR spectra were separately normalized on the basis of carbonyl absorption bands. As shown in Figure 6, there could detect five apparent different sites in the ATR-FTIR absorption at 2965, 1714, 1472, 1152, and 919 cm<sup>-1</sup> between the original and enzymatic degraded film samples.

According to the principles of ATR-FTIR,<sup>35,36</sup> it has been well-known that there is an incident wavelength dependence of detectable depth from the sample surface as

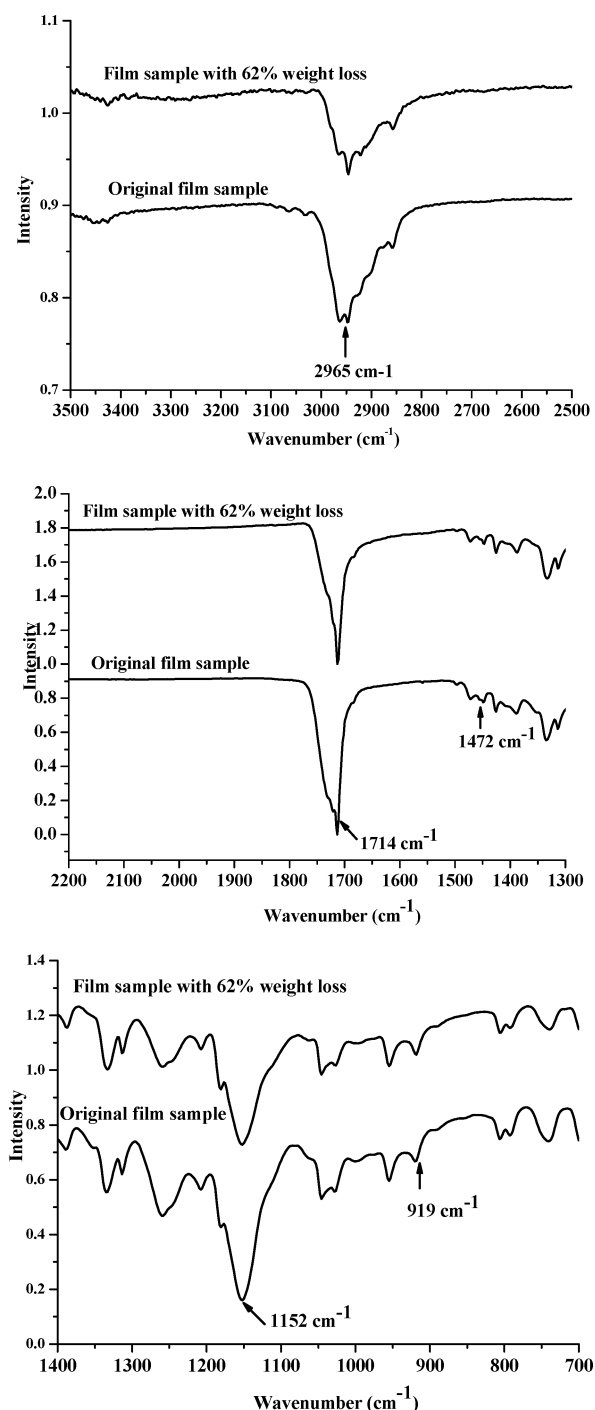
$$d_p = \frac{\lambda_1}{2\pi n_1 (\sin^2 \theta - n_{21}^2)^{1/2}} \quad (1)$$

where  $\lambda$  is the wavelength of FTIR incident light,  $n_1$  and  $n_2$  express refractive indexes of the ATR crystals and a film sample, respectively, and  $n_{21}$  is the ratio of  $n_2/n_1$ ,  $\theta$  is the incident angle,  $d_p$  is the detectable depth. In this study, the ATR-FTIR spectra were recorded with a KRS-5 crystal ( $n_1 = 2.38$ ) at an incident angle of 45°. Although the  $n_2$  of the P(BS-*co*-21.9 mol %BTMC) film sample was unknown, the physical properties of PBS and its macromolecular derivatives are similar to that of polyethylene or polystyrene.<sup>37</sup> For the purpose of qualitative characterization of the biodegradation behavior of P(BS-*co*-21.9 mol %TMC), in this study,  $n_2$  equal to 1.50 for polyethylene was tentatively applied. Thus, the equation 1 could be reduced as

$$d_p = \frac{1}{4.79\nu} \quad (2)$$

in which  $\nu$  means the parameter of wavenumber.

On the basis of eq 2, the ATR-FTIR absorption bands at 2965, 1714, 1472, 1152, and 919 cm<sup>-1</sup> were calculated to be relevant to the detectable depths  $d_p$  of 0.07, 0.12, 0.14, 0.18, and 0.22  $\mu$ m, respectively, demonstrating the surface initiated enzymatic degradation occurred in a depth 0.22  $\mu$ m. In addition, it is also noteworthy that the half-height width of the normalized carbonyl IR absorption band was found to reduce from the original 39 cm<sup>-1</sup> to a value of 27 cm<sup>-1</sup> when 62% of the film sample was enzymatic degraded. It has been reported that the higher degree of crystallinity was

**Figure 6.** ATR-FTIR spectra of the P(BS-*co*-21.9mol % BTMC) film samples before and after enzymatic degradation by lipase PPL.

for a bacterial poly(3-hydroxybutyrate-*co*-3-hydroxypropionate) sample, and the narrower carbonyl FTIR absorption band would be detected.<sup>38</sup> Therefore, the narrower half-height width of carbonyl ATR-FTIR absorption band substantiated



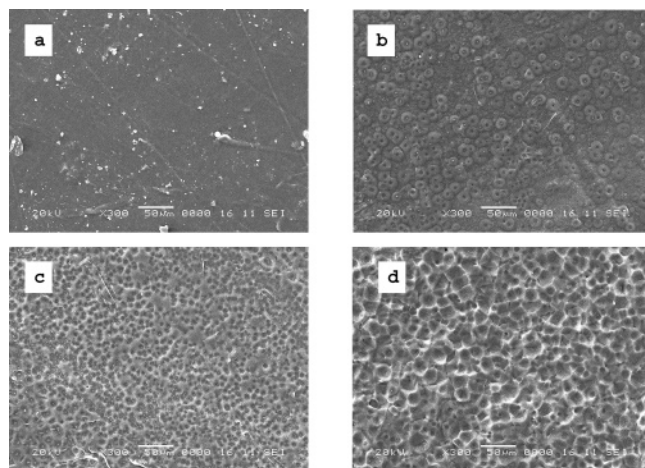


**Figure 7.** SEM morphological profiles of the original film (a), film sample with 40% weight loss (b), film sample with 62% weight loss (c), and film sample with 90% weight loss for the P(BS-co-21.9 mol %BTMC) (d).

a faster enzymatic degradation in the amorphous regions of the P(BS-co-21.9 mol % BTMC) film surface.

In an alternative way, morphological study on the lipase PPL degraded P(BS-co-21.9mol % BTMC) film samples was conducted via scanning electron microscopy (SEM), and the results are depicted in Figure 7. It can be seen that the original film sample exhibited a smooth surface, and morphologies of other three film samples (b~d) showed a clear evolution of porous surface structure along with the time of enzymatic degradation. Approximately, the averaged size of pores or cavities were calculated to be 2~5  $\mu\text{m}$  for 40% degraded film sample, and this was remarkably enlarged to 10~20  $\mu\text{m}$  when its biodegradability approached 90%, indicating a morphological evidence of surface initiated enzymatic degradation of the synthesized P(BS-co-CC) film samples.

**Cell Biocompatibility Assay of the New Synthesized P(BS-co-CC)s.** Assay of cell biocompatibility is a crucial and necessary work for a new synthesized biodegradable polymer toward the final biomedical and pharmaceutical applications. Up to date, there have already been a number of works published on in vitro and vivo cell biocompatibility and cytotoxicity assay and application of poly(L-lactide acid) PLLA as functional biomaterial.<sup>39</sup> In this study, cell biocompatibility assay using NIH 3T3 mouse fibroblast cell was conducted for the synthesized 11 P(BS-co-CC) samples bearing different functionalizable carbonate building blocks with regard to the cell adhesion and proliferation. In parallel, the experiment of a commercially available PLLA was concurrently done as the reference. Figure 8 presents the cytotoxicity assay of the synthesized new P(BS-co-CC) samples via the 3-(4,5-dimethylthiazol-2-yl)-2,5-diphenyltetrazolium bromide) MTT method, and it was indicated that the viabilities of NIH 3T3 mouse fibroblast cells seeded onto the substrates of the synthesized P(BS-co-CC)s exhibited final results similar to that for PLLA substrate, and there were no significant differences between the synthesized P(BS-co-CC) samples and PLLA reference in the MTT test ( $p > 0.05$ ). This suggests that most of the new synthesized P(BS-co-CC) samples exhibited as good biocompatibility as

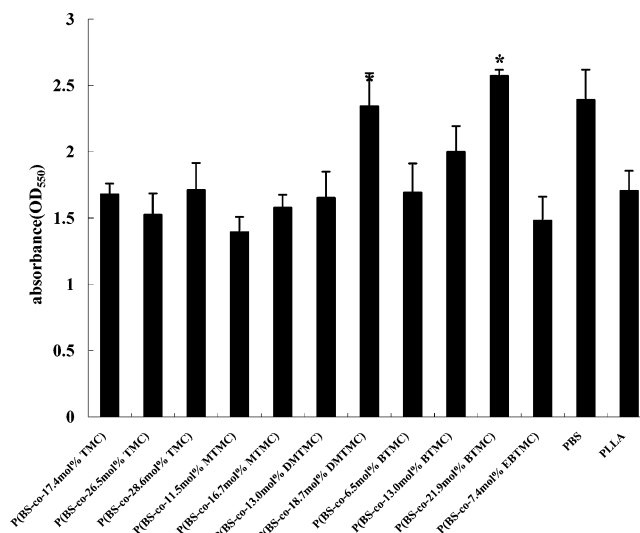


**Figure 8.** MTT assay of the NIH3T3 mouse fibroblast cell cytotoxicity on the film substrates of the P(BS-co-CC) as well as PBS and PLLA.

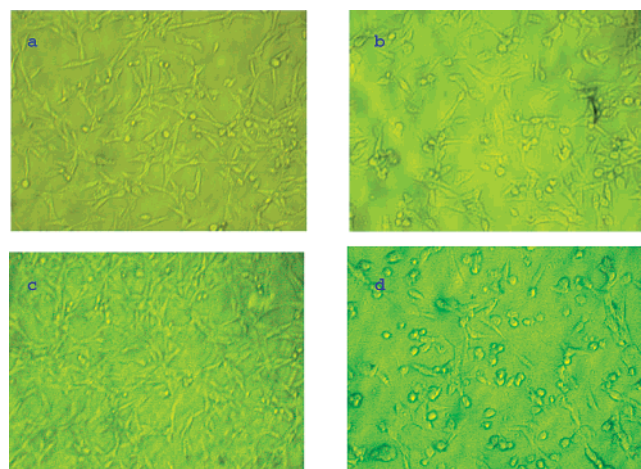


**Figure 9.** Morphologies of NIH 3T3 mouse fibroblast cell adhesion and proliferation on the film substrates: (a) PLLA, (b) P(BS-co-26.9 mol % TMC), (c) P(BS-co-18.7 mol % DMTMC), and (d) P(BS-co-21.9 mol % BTMC).

the well applied PLLA. Interestingly, the viabilities of NIH 3T3 mouse fibroblast cell cultivated on the substrates of the P(BS-co-18.7 mol % DMTMC) and P(BS-co-21.9 mol % BTMC) were found to be even much better than that of the PLLA reference, demonstrating better cell biocompatibility which could be obtained via tuning the carbonate building block.

Figure 9 shows the appearances of NIH 3T3 mouse fibroblast cells on the substrates visualized by optical microscope. It was seen that the cells cultivated on the substrate of poly (BS-co-28.6 mol % TMC) exhibited morphology as seen in Figure 9b similar to that of the PLLA. In contrast, the cells were clearly found to better spread on the P(BS-co-18.7 mol % DMTMC). In addition, SEM studies for the substrates after 48-h cell incubation as seen in Figure 10 showed much better apparent cell adhesion and proliferation for the P(BS-co-18.7 mol % DMTMC) and P(BS-co-21.9 mol % BTMC) than other copolymer samples, demonstrating their better biocompatibilities.

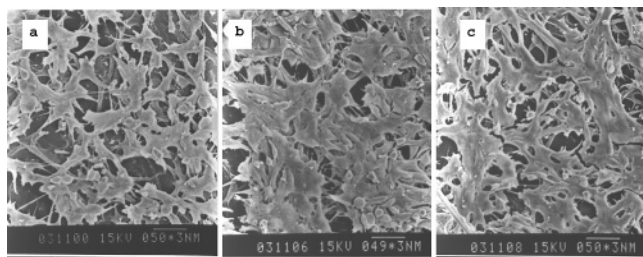


**Figure 10.** SEM micrographs of the NIH 3T3 mouse fibroblast cells on the film substrates of (a) P(BS-co-26.5mol %TMC), (b) P(BS-co-18.7mol %DMTMC), and (c) P(BS-co-21.9 mol %BTMC) after a 48-h cell incubation.

## Conclusions

On the basis of the synthesized novel aliphatic P(BS-co-CC)s bearing various functionalizable carbonate building blocks of TMC, MTMC, DMTMC, BTMC, EBTMC, in this study, the enzymatic degradation behavior of these copolymer film samples as well as the PBS sample was examined under 37 °C in the phosphate buffer solution (pH=7.4), containing lipase Novozyme 435 or lipase PPL. The biodegradation results by lipase Novozyme 435 indicated that the linear PBS could hardly be biodegraded while the film samples of P(BS-co-CC)s showed fast biodegradation, and the enzymatic biodegradation was regulated by the overall impacts of comonomer structure and molar content, molecular weight, thermal characteristics and so forth. Meanwhile, in the case of lipase PPL, only two film samples of P(BS-co-28.6 mol % TMC) and P(BS-co-21.9 mol % BTMC) were obviously biodegraded even after an experimental time scale of 25 days. Furthermore,  $^1\text{H}$  NMR, GPC analysis of the water-insoluble residual copolymer samples indicated there was no appreciable change in molar mass and comonomer content, and LC-MS results of the water-soluble products demonstrated the presence of monomeric and oligomeric fragments, depending on the different carbonate building blocks. Additionally, morphological studies by ATR-FTIR, SEM indicated that the enzymatic degradation initiated on the film surface and finally evolved to porous structure. On these evidences, an exo-type mechanism of enzymatic chain hydrolysis was suggested to initiate from film surface and preferentially occur in the noncrystalline regions as confirmed by the DSC and ATR-FTIR results. With regard to cell biocompatibility assay, NIH 3T3 mouse fibroblast cells were applied for investigation of the synthesized 11 P(BS-co-CC) samples as well as PBS as substrates with respect to the cell adhesion and proliferation. It was noteworthy that MTT cytotoxicity assay indicated that most of the synthesized new P(BS-co-CC) samples exhibited cytotoxicities similar to that of the PLLA reference, and the samples of P(BS-co-18.7 mol % DMTMC) and P(BS-co-21.9 mol % BTMC) interestingly showed much better cell biocompatibilities as compared with the PLLA control.

On the basis of these new biodegradable prospective poly(ester carbonate)s, Pd/C catalyzed hydrogenation of P(BS-co-BTMC) and P(BS-co-EBTMC), successive preparation of novel poly(ester carbonate)s bear tunable hydrophilic lateral hydroxyl groups and preliminary application as a steroid type of long-term antiinflammatory drug carrier are

now under investigation in our lab, and will soon be continued in a forthcoming work.

**Acknowledgment.** The authors are indebted to Mr. X. Wang of Novozyme Ltd, China for kindly providing the lipase of Novozyme 435, and the authors are also grateful to the important financial supports partially from the Hundreds of Talents Project, CAS, National Science Foundation of China (No.20204019), Shanghai Municipal Basic Research Fund (No. 02DJ14071).

## References and Notes

- (1) (a) Langer, R. *Science* **1990**, 249 (2), 1527. (b) Langer, R. *Acc. Chem. Res.* **1993**, 26, 537. (c) Mooney, D. J.; Baldwin, D. F.; Suh, N. P.; Vacanti, J. P.; Langer, R. *Biomaterials* **1996**, 17, 1417.
- (2) Ranade, V. V. *J. Chin. Pharm.* **1990**, 30, 10.
- (3) Jeong, B.; Lee, K. M.; Gutowska, A.; An, Y. H. *Biomacromolecules* **2002**, 3, 865.
- (4) Lu, L.; Peter, S. J.; Lyman, M. D.; Lai, H. L.; Leite, S. M.; Tamada, J. A.; Uyama, S.; Vacanti, J. P.; Langer, R.; Mikos, A. G. *Biomaterials* **2000**, 21, 1837.
- (5) Singh, M.; Shirley, B.; Bajwa, K.; Samara, E.; Hora, M.; O'Hagan, D. *J. Controlled Release* **2001**, 70, 21.
- (6) Asano, M.; Yoshida, M.; Kaetsu, I.; Imai, K.; Masnimo, T.; Yuasa, H.; Yamanaka, H.; Suzuki, K.; Yamazaki, I. *Makromol. Chem. Rapid Commun.* **1985**, 6, 509.
- (7) Colo, G. D. *Biomaterials* **1992**, 13, 850.
- (8) Langer, R.; Lund, D.; Leong, K.; Folkman, J. *J. Controlled Release* **1985**, 2, 331.
- (9) Zhu, K. J.; Hendren, R. W.; Jensen, K.; Pitt, C. G. *Macromolecules* **1991**, 24, 1736.
- (10) Fujimaki, T. *Polym. Degrad. Stab.* **1998**, 59, 209.
- (11) (a) Shirahama, H.; Kawaguchi, Y.; Aludin, M.; Yasuda, H.; *J. Appl. Polym. Sci.* **2001**, 80, 340. (b) Ishii, M.; Okazaki, M.; Shibasaki, Y.; Ueda, M.; Teranishi, T. *Biomacromolecules* **2001**, 2, 1267.
- (12) (a) Witt, U.; Müller, R. J.; Deckwer, W. D. *J. Macromol. Sci. Pure Appl. Chem.* **1995**, A32 (4), 853. (b) Witt, U.; Yamamoto, M.; Seeliger, U.; Müller, R. J.; Warzelhan, V. *Angew. Chem., Int. Ed.* **1999**, 38, 1438.
- (13) (a) Albertsson, A. C.; Eklund, M. *J. Polym. Sci. A: Polym. Chem.* **1994**, 32, 265. (b) Albertsson, A. C.; Eklund, M. *J. Appl. Polym. Sci.* **1995**, 57, 87.
- (14) Buchholz, B. *J. Mater. Sci. Mater. Med* **1993**, 4, 381.
- (15) Yasuda, H.; Aludin, M. S.; Kitamura, N.; Tanabe, M.; Shirahama, H. *Biomacromolecules* **1999**, 32, 6047.
- (16) Cai, J.; Zhu, K. J.; Yang, S. L. *Polym. Int.* **1996**, 41, 369.
- (17) Taniguchi, I.; Nakano, S.; Nakamura, T.; El-Salmawy, A.; Miyamoto, M.; Kimura, Y. *Macromol. Biosci.* **2002**, 2, 447.
- (18) Chen, X. H.; McCarthy, S. P.; Gross, R. A. *J. Appl. Polym. Sci.* **1998**, 67 (1), 547.
- (19) (a) Takata, T.; Igarashi, M.; Endo, T. *J. Polym. Sci. Part A: Polym. Chem.* **1990**, 29, 781. (b) Al-Azemi, T. F.; Bisht, K. S. *Macromolecules* **1999**, 32, 6536. (c) Vandenberg, E. J.; Tian, D. *Macromolecules* **1999**, 32, 3613. (d) Shen, Y. Q.; Chen, X. H.; Gross, R. A. *Macromolecules* **1999**, 32, 3891.
- (20) John, G.; Tsuda, S.; Morita, M. *J. Polym. Sci. Part A: Polym. Chem.* **1997**, 35, 1901.
- (21) Suggs, L. J.; Shive, M. S.; Garcia, C. A.; Anderson, J. M.; Mikos, A. G. *J. Biomed. Mater. Res.* **1998**, 46, 22.
- (22) Kirkpatrick, C. J.; Mittermayer, C. *J. Mater. Sci. Mater. Med.* **1990**, 1, 9.
- (23) Oliva, A.; Salerno, A.; Locardi, B.; Riccio, V.; Ragione, F. D.; Iardino, P.; Zappia, V. *Biomaterials* **1998**, 19, 1019.
- (24) Ratner, B. D. *Biomater. Sci.* **1997**, 453.
- (25) (a) Zhang, S.-P.; Yang, J.; Liu, X.-Y.; Cao, A. *Biomacromolecules* **2003**, 4, 437. (b) Yang, J.; Hao, Q.-H.; Liu, X.-Y.; Ba, C.-Y.; Cao, A. *Biomacromolecules* **2004**, 5, 209. (c) Zhang S.-P., Yang, J., Liu, X.-Y., Chang J.-H., Cao, A. *Chin. J. Org. Chem.* **2003**, 9, 1008.
- (26) (a) Ydens, I.; Rutot, D.; Degée, P.; Six, J. L.; Dellacherie, E.; Dubois, P. *Macromolecules* **2000**, 33, 6713. (b) Gohy, J. F.; Lohmeijer, B. G. G.; Schubert, U. S. *Macromol. Rapid Commun.* **2002**, 23, 555.
- (27) (a) Ringsdorf, H. *J. Polym. Sci., Part C, Polym. Symp.* **1975**, 51, 135. (b) Akashi, M.; Takemoto, K. *Adv. Polym. Sci.* **1990**, 97, 107.

- (28) (a) Tasaka, F.; Miyazaki, H.; Ohya, Y.; Ouchi, T. *Macromolecules* **1999**, 32, 6386. (b) Aoi, K.; Aoi, H.; Okada, M. *Macromol. Chem. Phys.* **2002**, 203, 1018.
- (29) Scandola, M.; Focarete, M. L.; Frisoni, G. *Macromolecules* **1998**, 31, 3846.
- (30) Sudesh, K.; Abe, H.; Doi, Y. *Prog. Polym. Sci.* **2000**, 25, 1503.
- (31) Kumagai, Y.; Kanesawa, Y.; Doi, Y. *Makromol. Chem.* **1992**, 193, 53.
- (32) Li, S. M.; Gerreau, H.; Vert, M. *J. Mater. Sci. Mater. Med.* **1990**, 1, 198.
- (33) Shirahama, H.; Umemoto, K.; Yasuda, H. *J. Biomater. Sci. Polym. Ed* **1999**, 10, 621.
- (34) Tsuji, H.; Ikada, Y. *J. Polym. Sci., Polym. Chem.* **1998**, 36, 59.
- (35) Ikejima, T.; Yagi, K.; Inoue, Y. *Macromol. Chem. Phys.* **1999**, 200, 413.
- (36) Ikejima, T.; Yoshie, N.; Inoue, Y. *Polym. Degrad. Stab.* **1999**, 66, 263.
- (37) Fujimaki, T. *Polym. Degrad. Stab.* **1998**, 59, 209.
- (38) Cao, A.; Ichikawa, M.; Ikejima, T.; Yoshie, N.; Inoue, Y. *Macromol. Chem. Phys.* **1997**, 198, 3539.
- (39) (a) Winet, H.; Bao, J. Y. *J. Biomed. Mater. Res.* **1998**, 40, 567. (b) Konno, T.; Kurita, K.; Iwasaki, Y.; Nakabayashi, N.; Ishihara, K. *Biomaterials* **2001**, 22 (13), 1883.

BM049705+